Measurement-Based Performance Evaluation of Advanced MIMO Transceiver Designs

Uwe Trautwein

MEDAV GmbH, Gräfenberger Strasse 32-34, 91080 Uttenreuth, Germany

TeWiSoft GmbH, Ehrenbergstrasse 11, 98693 Ilmenau, Germany
Email: uwe.trautwein@tewisoft.de

Christian Schneider

Institute of Communications and Measurement Engineering, Ilmenau University of Technology, 98684 Ilmenau, Germany
Email: christian.schneider@tu-ilmenau.de

Reiner Thomä

Institute of Communications and Measurement Engineering, Ilmenau University of Technology, 98684 Ilmenau, Germany
Email: reiner.thomae@tu-ilmenau.de

This paper describes the methodology and the results of performance investigations on a multiple-input multiple-output (MIMO) transceiver scheme for frequency-selective radio channels. The method relies on offline simulations and employs real-time MIMO channel sounder measurement data to ensure a realistic channel modeling. Thus it can be classified in between the performance evaluation using some predefined channel models and the evaluation of a prototype hardware in field experiments. New aspects for the simulation setup are discussed, which are frequently ignored when using simpler model-based evaluations. Example simulations are provided for an iterative ("turbo") MIMO equalizer concept. The dependency of the achievable bit error rate performance on the propagation characteristics and on the variation in some system design parameters is shown, whereas the antenna constellation is of particular concern for MIMO systems. Although in many of the considered constellations turbo MIMO equalization appears feasible in real field scenarios, there exist cases with poor performance as well, indicating that in practical applications link adaptation of the transmitter and receiver processing to the environment is necessary.

Keywords and phrases: MIMO systems, channel modeling, channel sounding, turbo equalization, link-level simulations.

1. INTRODUCTION

MIMO transmission schemes are attractive candidates for the new air interfaces of wireless networks beyond 3G. This is due to the expected increase in spectrum efficiency, which results from a simultaneous transmission of multiple data streams from different antenna elements [1]. The transmitted signals are intentionally not orthogonal in any of the conventional communication signal dimensions, that is, by time, frequency, or code. Conceptually, the multipath propagation of the radio channel gives rise to different spatiotemporal signatures for the different transmit data streams, which permits a receiver equipped with multiple antennas to separate those data streams from the received signal mixture. Keeping this in mind, it is not really surprising that the performance

of a MIMO system will strongly depend on the radio channel conditions. A key question for a system implementation is, therefore, do we find practically feasible schemes that are sufficiently robust for this task? Or somewhat related, what specific features are required for a practical MIMO system to work reliably under a wealth of various propagation conditions?

This paper approaches those questions by describing a realistic simulation methodology which is focused to gain insights into propagation-related effects of a specific MIMO transceiver design example. The idea is to use the results of double-directional real-time channel sounding experiments [2] for MIMO link-level simulations. Thus, the proposed method fills the gap between the conclusions obtained by idealized simulations based on some channel model and the results of using a prototype hardware in field experiments. The advantages of the measurement-based offline simulation in comparison with the prototype experiments are higher flexibility, lower costs, and an improved perception of the

---

transceiver's operation, which is primarily due to more effective analysis techniques. The paper does not investigate the detrimental effects resulting from practical implementation issues, although the proposed simulation method could be extended accordingly.

Many of the proposals for implementing MIMO systems consider only algorithms suitable for frequency-flat fading radio channels [3, 4]. This simplifies the channel modeling requirements significantly since only spatial correlations of the signals are to be considered. But for the expected high data rates of future mobile communication systems, frequency-selective fading channels are inevitable. The OFDM approach is frequently adopted in order to convert the wideband channel into a multitude of frequency-flat channels. It goes along with this idea that the channel modeling is often separated into the spatial and the frequency dimension, which in general does not reflect reality. Furthermore, in an OFDM system, multipath diversity can only be gained if the channel coding is explicitly designed to do so [5]. Joint space-time equalization in single-carrier wideband systems is in contrast inherently capable to exploit multipath diversity and to simultaneously suppress cochannel interference [6]. This motivates its consideration also for MIMO systems. Different promising proposals for numerically efficient signal separation methods for frequency-selective channels are based on iterative interference cancellation techniques. For example, in [7], the successive detection principle of the BLAST algorithm is extended. Especially for CDMA systems, several optimal [8] and suboptimal [9, 10] concepts for iterative multiuser receivers can be found. But it seems questionable whether the bandwidth expansion of CDMA systems is a viable option for future wideband systems. In contrast to this, the combination of parallel soft interference cancellation, minimum mean square error (MMSE) detection, and soft-input soft-output (SISO) channel decoding leads to an iterative turbo-detection scheme [11] suitable for single-carrier transmission, which is called a turbo MIMO equalizer (TME).

Wideband MIMO receivers depend on the joint spatial *and* temporal multipath structure at the transmitter (Tx) side as well as the receiver (Rx) side of the radio link. Hence, evaluating the performance of a wideband MIMO detection scheme by means of simulations requires much more detailed knowledge and exactness of the channel than conventional single-antenna systems or systems with multiple antennas only at one side of the link. This makes high demands on an appropriate MIMO channel model, which is currently a hot topic in the research. However, the validation of the different proposals is frequently relied on from the system design perspective rather abstract benchmark criteria, like the channel capacity [12, 13]. The corresponding outcome of a channel model, which is parameterized to a measured scenario, is thereto compared with the results from real measured data. Although the channel capacity seems to be the performance criterion *par excellence* when considering MIMO systems, this does not necessarily imply that a good match in modeling the capacity guarantees a sufficient match to model the spatiotemporal channel structure for a
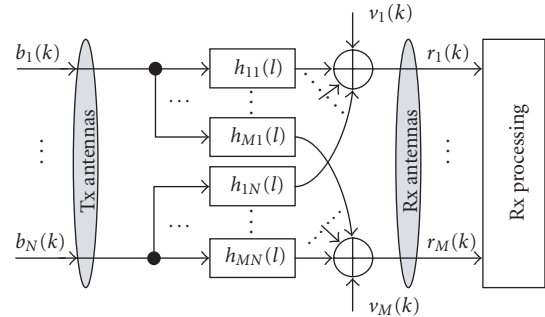

Figure 1: System model for MIMO transmission.

particular transceiver signal processing scheme. For this reason, a good practice is the validation of new models in terms of the performance results of system simulations. This is possible by comparing the model-based results with the results obtained when directly using the data of representative example environments, which requires that the model be parameterized to the measured data.

The paper is organized as follows. Section 2 describes the system model for a wideband MIMO system and presents a brief summary of the TME-based transceiver concept. Next, the MIMO measurement procedure and the methods for measurement-based link-level simulations are described. Simulation results for specific investigations and the connection to propagation analysis results are shown in Section 4. This extends initial results of [14]. Some conclusions are given in Section 5.

2. WIDEBAND MIMO SYSTEM

2.1. System model

The TME concept has been derived in [11], based on a proposal of an iterative CDMA receiver [9, 15]. This paper discusses its application for generalized MIMO system setups, which comprises a multiuser (MU) setup, a point-to-point (P2P) setup, as well as a multiuser MIMO setup. In order to simplify the description, the TME-based receiver is assumed at the base station (BS) of a cellular system or at the access point of a wireless local area network (WLAN) system. In the MU setup, the multiple transmit data streams originate from several single-antenna user terminals. The goal of adopting the MIMO approach in this setup is to maximize the system capacity in bps/Hz per radio cell. The P2P setup allows to maximize the link capacity in bps/Hz for a single link between a user terminal equipped with multiple antennas and the BS. The multiuser MIMO setup combines both features by allowing several user terminals with multiple antennas. Some implications of the different setups on the system design are discussed later. Here, it should only be mentioned that a coding scheme spanning multiple antennas is obviously only possible if they are located at the same terminal.

The system model for a general wideband MIMO system with N independent transmit data streams is depicted in Figure 1. The transmit data symbols $b_n(k)$ are taken from the respective modulation alphabet with the mean power normalized to $\sigma_b^2 = 1$. The radio channel between each pair

of the M receive and N transmit antennas is modeled by the complex finite channel impulse response $h_{mn}(l)$ having L taps. Thus, the receive signal at antenna m can be written as

$$r_m(k) = \sum_{l=0}^{L-1} \sum_{n=1}^{N} h_{mn}(l) b_n(k-l) + \sigma_v v_m(k), \qquad (1)$$

where $v_m(k)$ are the complex additive white Gaussian noise (AWGN) samples at receive antenna m with variance 1. The channel memory introduces intersymbol interference (ISI) to the transmit symbols, and the multiple simultaneous transmissions affect each transmit signal by cochannel interference, originating from all other signals. This is also denoted as multiple-access interference (MAI). For the detection process, the receiver uses a number of spatial and temporal receive signal samples which are stacked into one large space-time (ST) receive signal vector for notational convenience,

$$\mathbf{r}(k)$$
$$= [r_1(k) \cdots r_M(k) \cdots r_1(k+L-1) \cdots r_M(k+L-1)]^T. \qquad (2)$$

Likewise, the noise samples are stacked into a vector $\mathbf{v}(k)$. For simplicity, it is assumed that the number of temporal samples used for the detection is equal to the channel memory length, that is, all multipath components of a data symbol are captured. In this case, the vector of transmit data symbols contributing to $\mathbf{r}(k)$ is

$$\mathbf{b}(k) = [b_1(k-L+1) \cdots b_N(k-L+1)$$
$$\cdots b_1(k+L-1) \cdots b_N(k+L-1)]^T, \qquad (3)$$

and a compact matrix notation of (1) can be written in the form

$$\mathbf{r}(k) = \mathbf{H}\mathbf{b}(k) + \sigma_v \mathbf{v}(k) \qquad (4)$$

by introducing the ST MIMO channel matrix

$$\mathbf{H} = \begin{bmatrix} \underline{H}(L-1) & \cdots & \underline{H}(0) & \cdots & \mathbf{0} \\ \vdots & \ddots & \vdots & \ddots & \vdots \\ \mathbf{0} & \cdots & \underline{H}(L-1) & \cdots & \underline{H}(0) \end{bmatrix}, \qquad (5)$$

which is constructed from the spatial channel matrices $\underline{H}(l)$ for each delay tap l:

$$\underline{H}(l) = \begin{bmatrix} h_{11}(l) & \cdots & h_{1N}(l) \\ \vdots & \ddots & \vdots \\ h_{M1}(l) & \cdots & h_{MN}(l) \end{bmatrix}. \qquad (6)$$

For later reference, the ST transmit channel vectors $\mathbf{h}_n$ are introduced as

$$\mathbf{h}_n = [h_{1n}(0) \cdots h_{Mn}(0) \cdots h_{1n}(L-1) \cdots h_{Mn}(L-1)]^T, \qquad (7)$$

which are essentially the central N columns of the $\mathbf{H}$ matrix.

2.2. Turbo MIMO equalization

In a TME-based single-carrier system, the transmit data symbols $b_n(k)$ are the result of an independent transmitter processing for each of the corresponding source bit streams. A simple convolutional error correcting code is applied, the coded bits are interleaved and afterwards modulated. This paper considers BPSK, QPSK, 8-PSK, and 16-QAM as modulation schemes.

A simplified diagram of the turbo MIMO equalizer highlighting the combined soft interference cancellation (SC) and minimum mean square error filtering (MMSE) is shown in Figure 2. Both steps rely on computing the mean and the variance of each transmitted symbol on the basis of the modulation symbol alphabet and the bit *a priori* log-likelihood ratios (LLRs) $\boldsymbol{\lambda}^a[c_n(k)]$. These values can be obtained by soft-input soft-output (SISO) decoding of the received coded bits $c_n(k)$ [16]. The estimated mean $\tilde{b}_n(k)$ of the coded transmit data symbols is effectively a soft replica of the transmit symbols, which allows the soft cancellation of the ISI and MAI components in the received signal vector. This is to be performed for each substream n,

$$\mathbf{r}_n(k) = \mathbf{r}(k) - \mathbf{H}\tilde{\mathbf{b}}_n(k). \qquad (8)$$

The vector $\tilde{\mathbf{b}}_n(k)$ comprises all soft symbol replicas, except for the symbol of interest $\tilde{b}_n(k)$, which is set to zero. After the SC step, remaining ISI and MAI components are minimized by applying an instantaneous MMSE filter $\mathbf{w}_n(k)$ to the output of each of the N cancellers, $z_n(k) = \mathbf{w}_n^H(k)\mathbf{r}_n(k)$ [9, 11]. This is especially important for the first iteration, where the cancellation process is without effect due to the unavailability of *a priori* information. The solution to the MMSE optimization is derived in [9, 11], resulting in

$$\mathbf{w}_n(k) = [\mathbf{H}\boldsymbol{\Delta}_n(k)\mathbf{H}^H + \sigma_v^2\mathbf{I}]^{-1}\mathbf{h}_n. \qquad (9)$$

Here, $\mathbf{I}$ is the identity matrix of size (LM) and $\boldsymbol{\Delta}_n(k)$ is the covariance matrix of the estimated transmit symbols. Since statistical independence of the data symbols is assumed, this matrix is diagonal with entries $\text{var}\{\tilde{\mathbf{b}}_n(k)\}$ [16]. The MSE at the output of the MMSE filter can be reasonably approximated by a Gaussian distribution. This is the key for a low-complexity approximation of the *extrinsic* symbol probability which is required for each possible symbol of the actual modulation alphabet of size M_s. The results are arranged in the vector $\mathbf{P}_n^e(k)$. Following the derivation in [16, 17], the $\text{ld}(M_s)$ LLRs of the detected code bits in $\boldsymbol{\lambda}^e[c_n(k)]$ are estimated by jointly utilizing the vector of *extrinsic* symbol probabilities and the available *a priori* coded bit LLRs $\boldsymbol{\lambda}^a[c_n(k)]$ resulting in an iterative demapping. The interleavers Π and deinterleavers Π^{-1} are equivalent to the corresponding interleavers within the Tx processing.

Over multiple iterations, the reliability of the estimated coded data symbols $\tilde{b}_n(k)$ increases. Hence, the SC step is more and more perfect and the importance of the ST MMSE
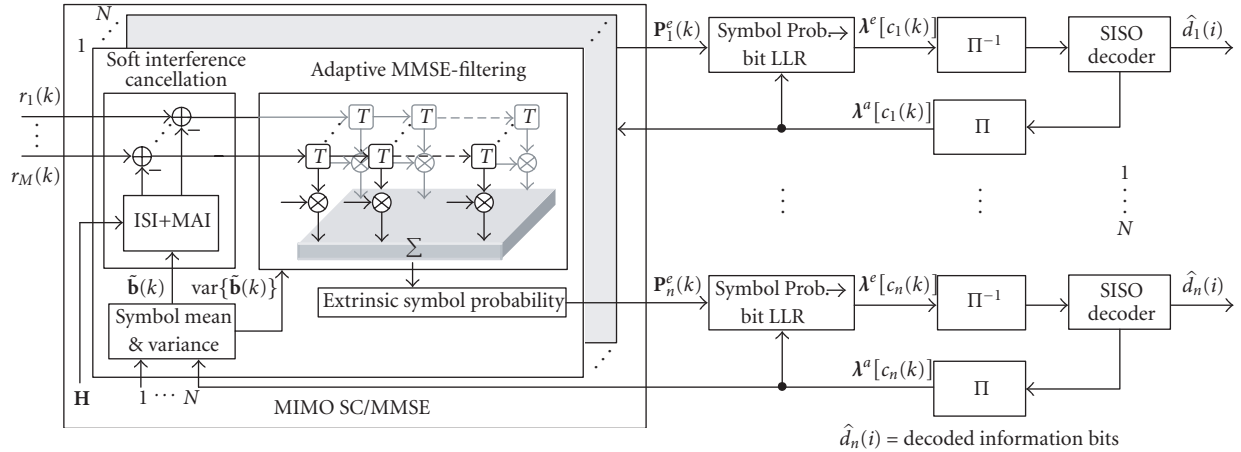
FIGURE 2: Turbo MIMO detector.

filter is reduced. In contrast, for the first iteration only the linear ST processing is responsible for separating the multiple cochannel signals. The required spatiotemporal selectivity depends on the number of receive antennas and a high degree of multipath diversity.

The computational complexity of the considered turbo MIMO equalization scheme can be regarded as low. The matrix inversion required for the calculation of the MMSE filter is the main complexity burden and grows only in cubic order with the number of parallel streams/users and their channel memory lengths. A comparable MLSE or maximum *a posteriori* (MAP) detection would result in an exponentially increasing complexity.

3. METHODS FOR MEASUREMENT-BASED LINK-LEVEL SIMULATION

3.1. *Realistic MIMO channel modeling*

Propagation modeling relies on a system-theoretic view on the wave propagation from the transmit antenna to the receive antenna. The wave propagation effects like scattering, reflection, and diffraction can be described by the complex channel impulse response. A statistical characterization of the impulse responses preserves the space-continuous nature of the electromagnetic wave propagation effects, but does not lead to an intuitive interpretation. A more descriptive representation is possible by approximating the wave propagation as a superposition of discrete partial waves [18, 19, 20]. Since the formation of the partial waves is related to an instantaneous physical constellation of the antennas and all other objects in the radio scenario, any change in the distance to be travelled by a partial wave leads to a Doppler shift in their complex amplitude. In a MIMO system, multiple antennas are placed in the wave field, which effectively carry out a spatial sampling of all the individual partial waves. Hence, an exhaustive description requires for each partial wave p the specification of the direction of arrival (DoA) at the receive antenna in azimuth and elevation (ψ_{R_p} and ϑ_{R_p}) and

equivalently the direction of departure (DoD) at the transmit antenna (ψ_{T_p} and ϑ_{T_p}), the propagation delay time τ_p, the Doppler shift α_p, and the complex amplitude matrix $\boldsymbol{\gamma}_p$, whose 2×2 entries quantify the co- and cross-polarization components. This yields the following signal model for the double-directional radio channel:

$$
\begin{aligned}
\mathbf{h}&(\alpha, \tau, \psi_R, \vartheta_R, \psi_T, \vartheta_T) \\
&= \sum_{p=1}^{P} \boldsymbol{\gamma}_p \delta(\alpha - \alpha_p) \delta(\tau - \tau_p) \delta(\psi_R - \psi_{R_p}) \\
&\quad \times \delta(\vartheta_R - \vartheta_{R_p}) \delta(\psi_T - \psi_{T_p}) \delta(\vartheta_T - \vartheta_{T_p}).
\end{aligned}
\tag{10}
$$

The identification of this model from measurements could be seen as the ultimate goal in propagation modeling, because it abstracts from a particular antenna and allows to derive all other types of channel models. The required procedures are very challenging. Thus, simpler approaches are frequently adopted.

Both deterministic and stochastic MIMO channel models have been proposed in the literature (see [21] for an overview), each with specific focus aspects and limitations. Their validation and, as the consequence thereof, modification are still a subject of intensive research. A lack of purely stochastic models is that a specific antenna characteristic is hard to incorporate. It seems that geometry-based models are a must [12, 22], but the wealth of required parameters makes their handling difficult. On the other hand, if for certain applications, the antenna selection is limited to some particular configurations, it is reasonably possible to derive statistical models including antenna properties. The prerequisite are channel measurements with those application specific antennas.

After introducing some facts on the measurement itself, it will be shown that the measurement data from representative sample environments can be of great benefit for transceiver design investigations.

3.2. *MIMO channel measurement*

A modern multidimensional channel sounder device like the RUSK MIMO [23] from MEDAV is capable to capture the channel characteristics for all dimensions involved in (10) completely in a Nyquist sense. The measurement principle is described in [2]. It relies on the transmission of a specialized periodic multifrequency test signal. Frequency-domain correlation at the receiver is employed to estimate the complex channel frequency response. Multiple antennas at the transmitter as well as the receiver side are managed by fast antenna multiplexing which is synchronized to the test signal period. A temporal sequence of MIMO snapshots of the channel thus yields a 4-dimensional data array D with dimensions (N_f, N, M, N_t), where N_f is the number of frequency samples within the measurement bandwidth B and N_t is the number of temporal samples collected during the observation time. In case of dual-polarized antennas, the numbers N and M include both polarization ports per antenna. For the extraction of the multidimensional path parameters in (10) from the measured frequency responses, high-resolution parameter estimation algorithms have been developed and successfully applied [24]. A mandatory prerequisite is the use of carefully designed measurement antennas.

The selection of suitable antennas is of specific importance, because it depends on the objectives of the measurement and the intended usage of the data. It should be emphasized that certain use cases can be mutually contradictory. For example, for investigations of space diversity processing, an antenna element spacing of multiples of the wavelength λ is usually desired. On the other hand, space coherent processing and high-resolution parameter estimation of the data is only possible if the element spacing is smaller than $\lambda/2$. The ability for a 3-dimensional resolution of the DoDs and DoAs is only possible if the array has an aperture in the horizontal as well as the vertical space dimension.

Another antenna related issue is the field of view both for the individual elements and the antenna array as a whole. Three possible combinations are relevant: in planar array structures (linear and rectangular arrays) the elements and the array cover only a sector. Circular arrays are constructed to have a 360° field of view with either directional elements (patch arrays, multibeam antennas) or omnidirectional elements (dipole arrays) [2].

A certain constellation of Tx and Rx antennas in a measurement campaign should always resemble one of the potential MIMO system setups introduced in Section 2.1. This implies consequentially the usable array configurations: directional arrays are typically mounted at the hypothetic BS position and antenna elements and/or arrays with omnidirectional coverage are utilized at the user terminal position. An element spacing in the order of several λ is usually an option for a BS array only. The large antenna spacings relevant to a multiuser scenario are mostly attained by a Tx side synthetic aperture principle, that is, by a sequential measurement of the individual user positions. Since both the propagation analysis and the performance evaluation are based on statistical averages, it is also important to collect
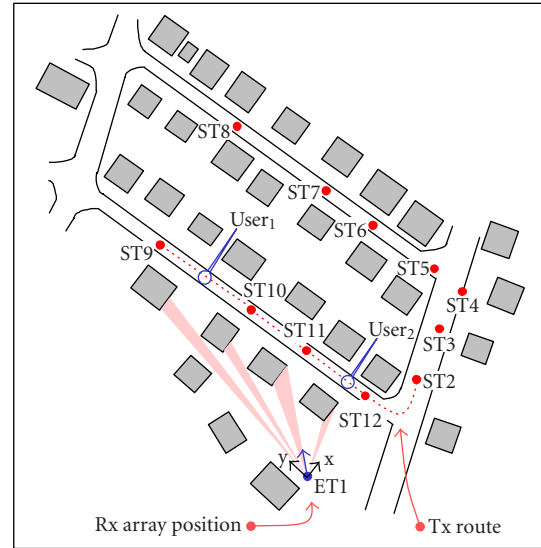

FIGURE 3: Measurement setup for a multiuser MIMO system.

a sufficient number of MIMO snapshots in each local surrounding. This is usually implemented by preferably equidistant measurements along predefined routes and/or repeated measurements in similar but yet distinct Tx/Rx constellations.

The layout of a measurement suitable for simulations of a multiuser system is depicted in Figure 3. The BS antenna, an 8-element uniform linear array (ULA) with 0.4λ element spacing, sits at an elevated position in a residential area, somewhat below the roof tops. The user terminal, equipped with a single omnidirectional antenna, travelled along several routes throughout the scenario. An approximately constant speed together with a high measurement rate ensured a spatial sampling grid of about 0.2λ, permitting the formation of a synthetic Tx array aperture down to relatively small extents. For the Tx positions along the route from ST9 to the indicated User 2 position, the line-of-sight (LoS) is obstructed, but strong reflections can be observed via the house fronts as indicated by the shaded sectors. This can already be recognized from the shape of the delay profiles of which Figure 4 shows an example. In the sequel, two different approaches are described in order to derive the channel coefficients on the basis of measurements in a real field scenario.

3.3. *Data-based channel modeling (DBCM)*

The DBCM method derives the channel coefficients $h_{mn}(l)$ in (1) directly from the measurement data array D.[1] The following discussion describes a few aspects to be considered for this method. The minimum analysis requirement is to verify the data for a sufficient signal-to-noise ratio (SNR). In a low SNR constellation, the measurement noise peaks act like multipath components in the simulation. Hence, those data have to be sorted out. Important as well is the limitation of

---

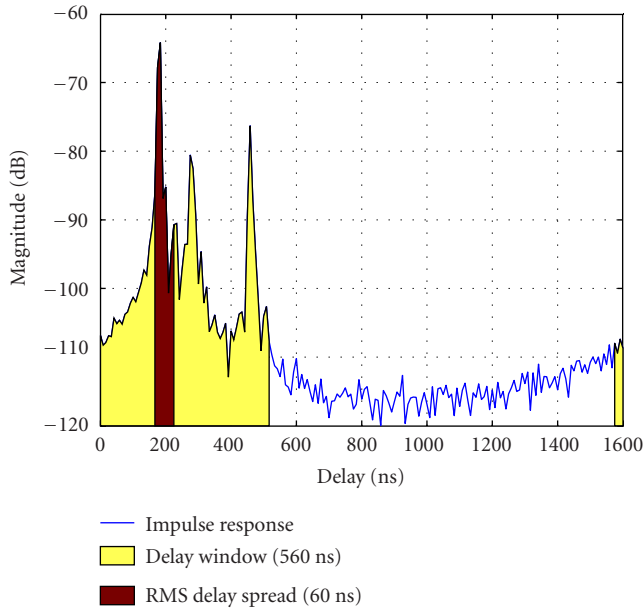[1]Appropriate sample data can be downloaded free of charge from [23].

FIGURE 4: On delay window selection. Example impulse response from the scenario in **Figure 3**. In order to reduce sidelobes, it is computed with a Hanning window of 120 MHz bandwidth.

the delay range of the impulse responses to the effective delay window. This denotes the delay span containing significant multipath energy. As indicated by the light-shaded area in Figure 4, it is usually much larger than the well-known RMS delay spread value. The measurement noise outside the delay window virtually introduces additional noise in the simulation. Thus, it is important to ensure a reasonable ratio of the measurement SNR and the maximum target SNR in the simulation. The delay window selection serves the additional purpose to compensate the base propagation delay. In a transmission system, this is the task of a rough delay control, for example, by means of an adaptive timing advance of the terminals. Since a frequency-domain measurement method is applied, basic Fourier transform properties are to be considered during the measurement and the data processing. Therefore, changes of the base propagation delay during the observation time can also lead to a cyclic shift of multipath components with respect to the measured delay interval (cf. **Figure 4**). The base delay compensation must take this problem into consideration. Another Fourier-related processing requirement is to use window functions with a smooth tapering for selection operations in the delay as well as the frequency domain, in order to prevent excessive sidelobes in the respective transform domain. This is most easily accomplished by integrating the pulse shaping filter at the Tx and the receive filter of the system to be simulated into the preprocessing. They are frequently designed to yield a total frequency response with a raised cosine shape, which meets the requirement of a smooth tapering. Absorbing Tx and Rx filters into the channel impulse response is also required to derive the channel coefficients with symbol rate tap spacing. This simplifies the simulation, because the

subtleties of symbol timing recovery can be excluded when the respective implementation issues are beyond the scope of investigation. Using a raised cosine filter with rolloff factor β results in a channel bandwidth of $(1 + \beta)$ times the symbol rate f_S. Since the measurement bandwidth is usually much larger (e.g., 120 MHz), a subband corresponding to the channel bandwidth is extracted and weighted by the raised cosine filter. The resulting impulse responses are afterwards subsampled to a sampling rate equal to f_S. A simple maximum energy criterion can be used to determine the optimum subsampling phase. It is important to note, that the length of the combined filter and channel response is the sum of the delay window length and the length of the raised cosine filter. The length of the filter again must be chosen the longer, the smaller its rolloff is. For a small β, this effect can be quite severe and requires careful consideration when designing a systems equalizer length or guard interval.

It has already been stressed that the antenna configuration is of exceptional relevance to MIMO systems. Although DBCM lacks the flexibility to incorporate arbitrary antenna properties after the measurements have been completed, a few interesting options for antenna variations should be discussed. Using a channel sounder, it is only of little expense to repeat similar measurements with a small number of different prefabricated antenna arrays, which have only a single-antenna port due to the built-in antenna multiplexer. Fastening individual antenna elements on a flexible holder allows easy changes in the geometrical arrangement and the element spacing as well. The multiplexing principle gives to a great extent flexibility in the number of elements, and this is why it is possible to measure with significantly more elements than it is intended in an actual transceiver design. This is frequently the situation if specialized measurement antennas for DoA/DoD estimation are employed. The following discussion will give an impression on that. A uniform rectangular array of 8×8 elements with $\lambda/2$ spacing has been designed to enable joint azimuth and elevation of arrival estimation of coherent multipath components with a resolution of $5°$. For the simulation of a 4×4 MIMO system, this allows to select antenna subsets in order to mimic various transceiver arrays with either horizontal and/or vertical aperture dimension as well as variable element distances of integer multiples of $\lambda/2$. Moreover, by combining the frequency responses of multiple elements in a row (column), the resulting element's beam width in elevation (azimuth) can be reduced and thus the antenna gain increased. Assuming that the array is properly calibrated, the resulting beam patterns can even be tilted by applying the required complex amplitude weights to the elements to be combined.

3.4. Measurement-based parametric channel modeling (MBPCM)

This method belongs like DBCM to the category of deterministic channel models. It is based on characterizing the wave propagation in a particular measurement environment by a finite number of discrete partial waves as in (10). Thus it is a two-step procedure with a parameter estimation step and a synthesis step [19]. Since the underlying model does
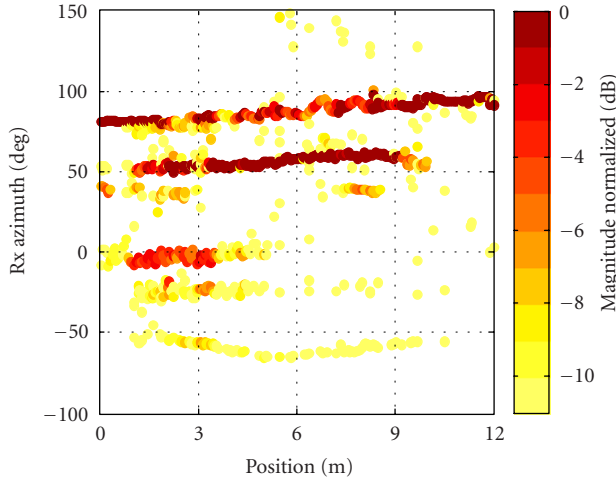
FIGURE 5: Estimated Rx azimuth of arrival of the multipath components observed for a walk along a street.

not depend on specific antennas, this model allows to consider the antenna-related effects in the synthesis step.[2] This increases the flexibility for system design-oriented simulations significantly, because the antenna setup can be easily varied.

An example result of the parameter estimation step of this method is given in Figure 5. It shows the Rx azimuth of arrival and the relative path weight observed within a section of a measurement drive along a street where the LoS between Tx and Rx was frequently obstructed by parking cars. Since the path parameters together with the complex amplitude of each path describe the wave field around the Tx as well as the Rx antenna arrays, they can be used to make a synthesis of MIMO impulse responses for different antenna array shapes than that of the measurement arrays. Even a variation of the array position in a small surrounding of a few λ or a change of the orientation is possible. Assuming plane wave fronts and only one polarization component, the synthesis can be performed by using

$$h_{mn}(l) = \sum_{p=1}^{P} \gamma_p g(lT - \tau_p) a_{T_n}(\psi_{T_p}, \vartheta_{T_p}) a_{R_m}(\psi_{R_p}, \vartheta_{R_p}),$$

(11)

where γ_p is the complex path weight of path p with delay τ_p and a_{T_n} is the nth element of the Tx array response vector in azimuth and elevation of the system antenna to be simulated. Likewise the Rx array response is contained in a_{R_m}. The array response may also contain a nonhomogenous directional element characteristics. $g(t)$ is the continuous-time impulse response of the combined transmit and receive filters, which is sampled in multiples of the symbol period $T = 1/f_S$. It has

---

[2]An obvious limitation is that the field of view of the measurement antennas is larger than or equal to the field of view of the antennas in the synthesis step and the required aperture dimensions are covered.

the same function like in the DBCM method and a raised cosine filter is usually applied.

Novel results extend the MBPCM method to include diffuse scattering components by superimposing a stochastic part whose characteristic parameters are estimated from the measured data as well [25].

3.5. System specific aspects of link-level simulations

The use of measured channel data in the simulation requires the consideration of some basic real-world transceiver functions. A simplified implementation, based on *a priori* knowledge, is desirable and legitimate, as long as the corresponding transceiver function itself is not to be examined. In model-based simulations, most of this functionality is not required, because the channel models are usually adapted to the transmission system and abstract the physical propagation background. Three aspects are discussed below that have to be considered in the context of a specific system design.

The system model introduced so far always assumed a time-invariant channel. This is a reasonable standard assumption for a wideband system with burst-oriented transmission. The following simple calculations motivate this: the channel can be approximated time-invariant over one burst, if the carrier phase uncertainty $\Delta\phi_c$ due to the Doppler effect is negligible over the burst duration. This can be expressed by the product of the Doppler bandwidth B_D and the burst duration T_B, $\Delta\phi_c = 360° \cdot B_D \cdot T_B$. On the one hand, the expected Doppler bandwidth increases with the system's carrier frequency and the supported maximum speed of the terminals. On the other hand, the higher the data rates, the shorter the burst duration for a typical amount of data symbols. For the example simulations in Section 4, the following numbers give an illustration: the maximum supported terminal speed should be 10 km/h, yielding a Doppler bandwidth of ± 48 Hz at 5.2 GHz carrier frequency. The assumed maximum number of data symbols per burst and antenna (including coding) is 2048 symbols, hence the burst duration at 20 Msymbols/s (Msym/s) is 102.4 microseconds. Consequently, $\Delta\phi_c = \pm 1.8°$, which is small compared to the data symbol's phase separation in all considered symbol alphabets.

The measured impulse responses have usually a significantly longer delay window (cf. Figure 4) than the temporal memory length of the receivers $T_R = LT$. Hence, a delay control must ensure that the receiver processing is temporally synchronized to that portion of the delay profiles offering the optimum performance. This task is similar but not identical to the problem of the delay window selection during the data preprocessing described in Section 3.3. Given the channel coefficients $h_{mn}(l)$, the delay control determines the start of the delay span of length T_R containing the maximum energy. For the P2P setup, all coefficients are spatially averaged to obtain one single delay control value. For the MU setup, each users coefficients are averaged to obtain one delay control value per user.

The power control is responsible for adjusting the desired receiver signal-to-noise ratio (SNR). For the MU setup, an ideal power control adjusts the transmit power at each

transmit antenna such that the mean received power over all elements is identical for all users, $\sum_{m=1}^{M} P_{mn} = M/N$. While this holds constant the total transmit power independently of the number of users, the total received power increases with the number of receive antennas. This is a pragmatic rule, which keeps the spirit behind the MIMO theory to increase the channel capacity by adding parallel channels at constant transmit power, while retaining the physical fact that the total received power increases with the number of antennas located in an electromagnetic field of a given strength. For the P2P setup, a modified power control scheme with lower complexity seems attractive, which adjusts the total received mean power while transmitting identical powers by each antenna, $\sum_{m=1}^{M} \sum_{n=1}^{N} P_{mn} = M$. But it has been found that this scheme introduces partially a serious performance degradation of the TME-based system.

4. SIMULATIONS FOR REAL FIELD SCENARIOS

This section covers by means of examples the strategies to evaluate the bit error rate (BER) performance of systems based on the TME concept as introduced in Section 2.2. The focus lies on characterizing the robustness w.r.t. varying propagation conditions and the influence of several design options. All simulations are based on measured channel data at 5.2 GHz carrier frequency. The assumed symbol rates are 12 Msym/s ($\beta = 0.5$) in case of the MU scenarios and 20 Msym/s ($\beta = 0.25$) for the P2P scenarios. Each data stream of the TME system is convolutionally encoded (code rate 1/2, constraint length 3, G = [7, 5]) and random interleaved. Gray mapping is used to derive the symbol constellations of the higher modulation schemes. On the receiver side, the channel decoding part was performed by the max-log-map algorithm [26].

4.1. Result evaluation basics

The outcome of link-level simulations are usually mean BERs averaged over a certain number of statistical realizations of the radio channel. In measurement-based simulations, those realizations are essentially obtained by changing the antenna positions in the scenario. Meaningful average BER results can only be expected if the averaging is carried out over channel realizations with similar statistics. For single antenna systems the assertion of statistical stationarity of the channel is relatively simple, because only the delay- (or frequency-) domain statistics needs to be observed. For MIMO systems, this task is much harder, since the spatiotemporal structure among the multiple transmit channels needs to be considered. The parametric channel estimation as already introduced above is very valuable, since it enables a matching between the instantaneous physical propagation conditions and the performance of a certain receiver configuration. The example in Figure 5 shows that even within only a few meters the propagation conditions can change dramatically, with just as dramatic implications on the receiver performance. The second simulation example in Section 4.2 and the examples in Sections 4.3 and 4.4 illustrate the effect of selective failures for certain Tx-Rx constellations. Here, the BER is high even at high SNR, or it is significantly higher than in very similar constellations. Selective failures are typically not produced in channel model-based simulations. A reasonable strategy to deal with this effect is needed in order to maintain valuable average performance conclusions. The strategy depends on the desired utilization of the simulation results. The exclusion of a certain percentage of worst case constellations might be an option.

On the other hand, those selective failures give a strong motivation for investigating link adaptation schemes and criteria for an operational system. Link adaptation schemes for MIMO system have to consider options that go beyond the traditional adaptive modulation and coding selection. This may comprise the adjustment of the number of parallel transmit signals, incremental coding, or the selection of antenna subsets according to a specific propagation situation.

4.2. Variable antenna configurations

The first example illustrates the basic performance behavior of the iterative MIMO transceiver scheme in a P2P scenario. The MBPCM method has been used to synthesize the MIMO channel coefficients based on the multipath parameters estimated from measured data. The parameters have been inspected to select a short section of the route displayed in Figure 5 with a stationary multipath situation (positions from 1 m to 3 m) and a particularly high delay spread (75 nanoseconds). Figure 6 shows the average BER over 15 channel snapshots of the selected section. The simulations have been carried out with 4 simultaneous BPSK transmit signals and 4 receive antennas (4/4 MIMO system). Uniform circular arrays (UCA) at both the receiver and the transmitter with omnidirectional antenna elements and $1.0\,\lambda$ spacing have been assumed. The receiver uses $L = 7$ delay taps per antenna element. An impressive gain can be obtained by performing multiple iterations of the receiver processing.

The second example extends the previous one by investigating the robustness of the 4/4 MIMO system with respect to a variable Rx antenna element spacing as well as the geometrical orientation of the Tx array. This combination is motivated by observing that the Rx azimuth spread in the considered section is with about 30° significantly smaller than the Tx azimuth spread of about 50°. A fixed element spacing of the Tx UCA of $1.0\,\lambda$ has been assumed, the Tx orientation is changed by rotating the array in steps of 22.5° (i.e., orientation 5 is identical to orientation 1), and the Rx element spacing is varied between $0.25\,\lambda$ and $1.0\,\lambda$. Figure 7 shows the BER for each constellation at an SNR of 5 dB. The first Tx array orientation yields a significantly higher BER than all others and shows a clear advantage for higher Rx element spacings. Turning the Tx array reveals the existence of an optimum around orientation 3 with a U-shaped increase on either side. This indicates that the effective number of multipath components in this scenario is too small to ensure the separability of the 4 transmit signals for every antenna constellation. Hence, the specific superposition of the multipath components at the different antenna positions has
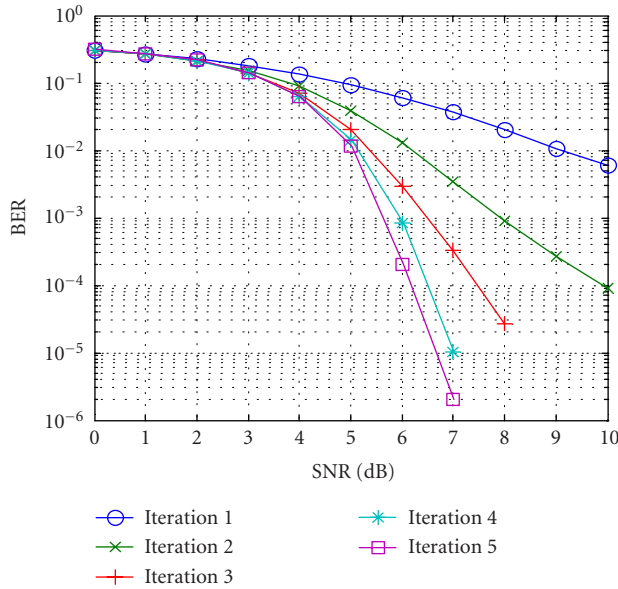
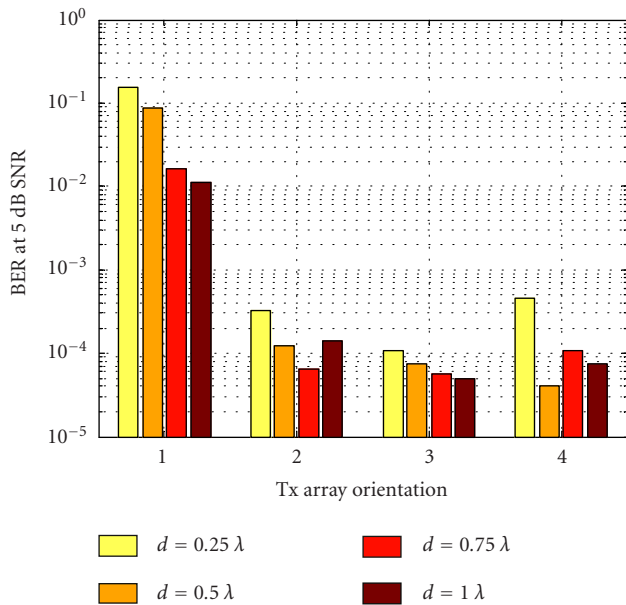FIGURE 6: Iteration gain for a 4/4 TME using UCAs with $1.0\,\lambda$ element spacing.

FIGURE 7: Effects of variable Rx element spacing and Tx array orientation for a 4/4 TME after 5 iterations.

an influence on the achievable BER. This issue will be taken up again in Section 4.4.

4.3. Position-variant BER analysis

The close relationship between the multipath characteristics and the BER performance is described in Figure 8 for the measurement route drawn in Figure 3. The simulation results for this and all subsequent figures are obtained using the DBCM method. The Rx antenna element spacing of the
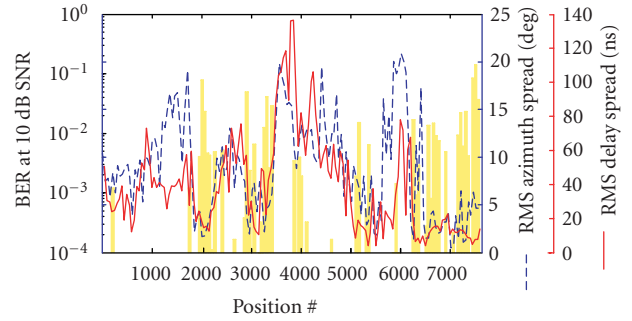

FIGURE 8: Interrelation of the position-variant BER (shaded bars) and the azimuth and delay spread along the route from ST9 to ST12 in Figure 3 (3/3 TME in a P2P setup, 4 iterations, 10 dB SNR).

simulated MIMO system is $1.2\,\lambda$, obtained by selecting 3 elements of the measurement ULA. The bit error rate of a 3/3 TME in the P2P setup with a transmit antenna spacing of approximately $1\,\lambda$ is shown as a bar chart and the RMS delay and azimuth spread values for the transmit positions are indicated by the lines. The received SNR is held constant for all positions. The observation is that for positions with low spread values, the receiver frequently shows a large BER or even a failure. Vice versa, in sections with significant multipath spread values, the BER is near zero.

For the implementation of a real communications system, it can be concluded from this observation that a link adaptation is required to maintain an efficient connection. By looking at the spread values along the route depicted in Figure 3, it is noticeable that in the considered microcellular scenario there exists no clear correlation between the Tx-Rx separation and the delay and azimuth spread. Further data analysis revealed likewise no clear correlation of the spread values with the received power. Hence, more sophisticated link adaptation criteria than the received SNR need to be elaborated.

4.4. Small-scale antenna displacement

The results in this section highlight the performance sensitivity of a 2/2 TME system regarding small antenna displacements. Furthermore, the influence of employing identical (Π_1) or different (Π_2) interleavers for the detection of two QPSK modulated transmit signals is depicted. The selected P2P MIMO measurement can be classified as a microcell outdoor scenario for a WLAN application with low mobility. A detailed description can be found in [23, 27]. The measurements were performed utilizing a UCA consisting of 16 omnidirectional elements as the Tx antenna. According to the small sketch illustrated in Figure 9, 16 different subsets are available consisting of two closely spaced elements (distance of $0.38\,\lambda$). From subset to subset, the two elements are changed only by one antenna position. On the receive side the two outer elements (distance of $3.46\,\lambda$) of an 8 element ULA were selected for the simulations. The position of this antenna was fixed, whereas the transmitter was passing at a distance of 10 meters under a transition from
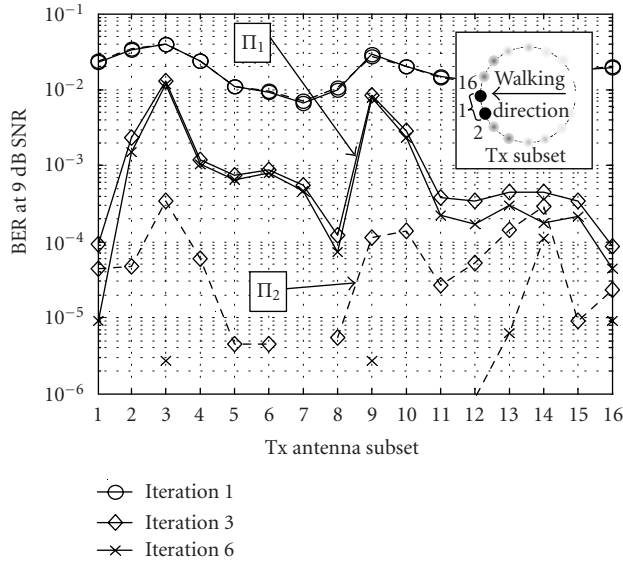
FIGURE 9: Effects of small antenna displacements on the performance of a 2/2 TME.

FIGURE 10: Performance of a 3/3 TME for various modulation schemes and different numbers of delay taps.

NLOS to LOS propagation conditions. For the simulations, 201 snapshots along the measurement track were selected and the SC/MMSE equalizer was equipped with $L = 5$ delay taps.

The continuous small antenna displacements over the entire UCA show considerable performance differences for the TME with identical interleavers. In Figure 9, the BERs are shown for each subset at 9 dB SNR. For the Tx subsets no. 3 and 9, the transmission completely failed, but subsets 8, 16, and 1 showed reasonable BERs. In general, for all Tx subsets, the final detection results are reached after three iterations and additional iterative processing shows no further improvements. Considering that the antenna displacements follow a circular shape and observing the course of subsets with low and high BERs, it seems that the same distinct directional propagation effects cause the similar results for equally oriented Tx subsets.

The TME utilizing different interleavers shows significantly better performance with an increasing number of iterations. This can be explained as follows: the similarity of the power delay profiles for each transmit antenna tends to produce erroneous received symbols at the same positions within the two transmit streams to be detected. In a TME with different interleavers, the resulting error sequences at the input of the channel decoders are differently permuted within the two streams (see Figure 2). Hence, the computation of the *extrinsic* soft information by the channel decoders is based on different temporal *a priori* reliability patterns in the two streams to be decoded. According to the information-theoretic comprehension of turbo equalization/decoding, the iterative processing gain strongly depends on the exchange of *extrinsic* information between the SC/MMSE equalizer and the SISO decoders. For the MIMO case, this comprises always the additional *extrinsic*
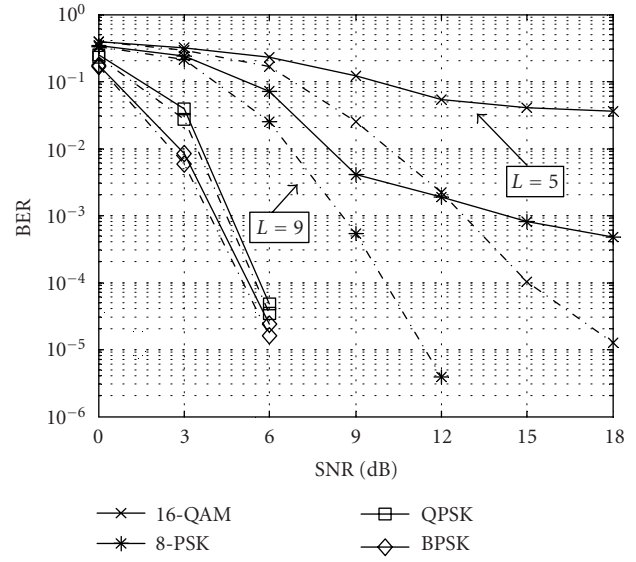
information of the respective other streams. The computation of this *extrinsic* information is more effective if the independence between the streams is increased by using different interleavers.

4.5. Modulation schemes

Based on the NLOS part (60 snapshots) of the MIMO channel considered in Section 4.4 the performance of a 3/3 TME with the different modulation schemes BPSK, QPSK, 8-PSK, and 16-QAM is evaluated. Additionally, an investigation of the impact of using different numbers of delay taps ($L = 5$ and $L = 9$) for the receiver's equalizer is carried out. All simulations utilize different interleavers for the transmit signals and the amount of symbols per transmit stream (512) is held constant. Hence, the effective number of information bits depends on the considered modulation. After 6 iterations, the results in Figure 10 show clearly that a parallel transmission of three independent 16-QAM modulated signals in the considered MIMO channel can be successfully performed with the TME concept using 9 delay taps for equalization. Furthermore, it is discovered that the same BER results can be gained for the BPSK and QPSK cases, regardless of using an equalizer with 9 or only 5 delay taps. But for the 8-PSK and 16-QAM modulation, a remarkable gap between the curves for the different equalizer lengths is observed. The feasibility of the SC/MMSE equalizer to capture the signal energy which is spread in the delay domain of the channel has significantly increasing influence with an increasing modulation alphabet.

4.6. Interleaver selection and Rx element spacing

Figure 11 summarizes simulation results for 100 snapshots of a multiuser MIMO setup in the residential area depicted
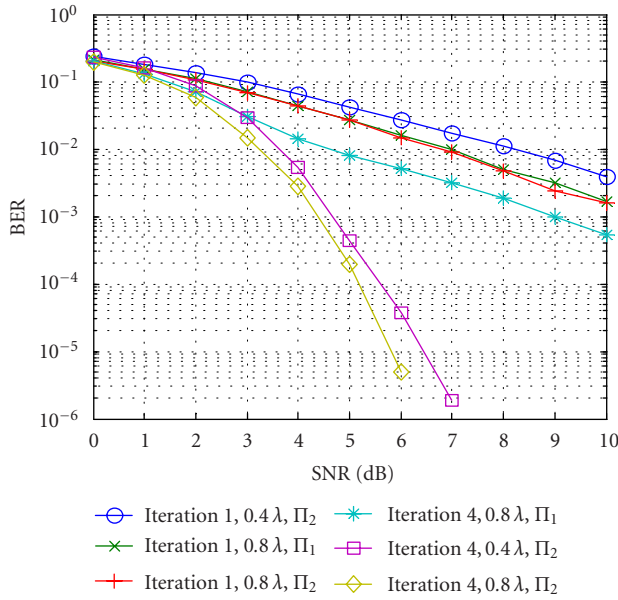
FIGURE 11: Average BER performance of a multiuser MIMO system (2 users with 2 Tx antennas each/4 antennas at the BS site).

FIGURE 12: Influence of the channel estimation on the performance of a 2/2 MIMO system (average of 100 snapshots of the route in Figure 3).

in Figure 3. Each of the two user terminals is equipped with 2 antennas with an element spacing of 1λ and transmits 2 BPSK modulated signals. The receiver features 4 elements of a uniform linear array with either 0.4λ or 0.8λ element separation. A reasonable BER performance in this constellation can only be achieved if a different interleaver is used in each of the 4 transmit streams (Π_2). Using identical interleavers (Π_1) leads to selective failures at some positions, which give rise to the relatively bad average BER performance. The difference is clearly only visible after performing the iterative detection process. In contrast, a smaller Rx antenna element spacing reveals a minor performance degradation for all iterations.

4.7. Channel estimation

All previously presented simulation results assumed that the ST channel matrix **H** is ideally known to the receiver. A real receiver must perform the channel estimation before it can start the detection. Estimation errors will introduce an additional performance degradation which has been investigated by simulating a realistic channel estimation scheme that relies on the transmission of training symbols in all Tx channels simultaneously at the beginning of a data burst. The estimator jointly estimates the vector of impulse responses from all N transmit antennas to one receive antenna $\bar{\mathbf{h}}_m = [h_{m1}(L-1)\cdots h_{mN}(L-1)\cdots h_{m1}(0)\cdots h_{mN}(0)]^T$, which is essentially the mth row of the matrix **H** transposed. A corresponding MMSE optimization criterion is given by

$$\bar{\mathbf{h}}_m = \underset{\bar{\mathbf{h}}_m\in\mathcal{C}^{NL}}{\arg\min}\, E\{||r_m(k) - \bar{\mathbf{h}}_m^T\mathbf{b}'(k)||^2\}, \qquad (12)$$

where $\mathbf{b}'(k)$ consists of the first NL elements of the vector $\mathbf{b}(k)$ introduced in (3). During the training phase of a burst
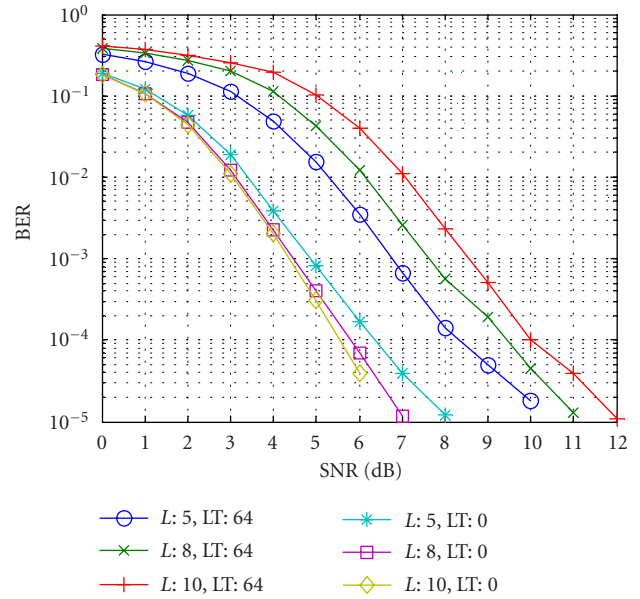
the $\mathbf{b}'(k)$ are known to the receiver. An adaptive solution of the optimization problem has been implemented by using the recursive least-squares (RLS) algorithm. Figure 12 compares the BER performance that can be achieved for a 2/2 MIMO system in a MU scenario with an ideally known channel (LT: 0) with that of a system using channel estimation based on 64 training symbols (LT: 64). Additionally, different numbers of temporal taps of the receiver are considered. The curves for the case of a known channel show a small advantage for receivers with a larger number of temporal taps. This situation is reversed for the curves including channel estimation, since the remaining estimation error depends on the ratio of the numbers of RLS iteration to the numbers of temporal taps, which varies between 12 for $L = 5$ and 5.5 for $L = 10$. Since the required number of training symbols is relatively large, the proposal of [11] for performing iterative channel estimation has also been applied successfully to real field data. For that purpose, additional reference data are obtained at higher iterations by using reliably detected data symbols as additional reference data. This scheme permits reducing the number of transmitted training symbols at the price of a higher number of turbo iterations.

5. CONCLUSIONS

For a successful MIMO system development, more efforts than ever before have to be spent on the channel modeling side, because the multipath propagation itself turns into a key component of the transmission system. Realistic models are extremely complex [22] and still under investigation. More open issues exist for the modeling of transitions from one propagation situation to another, for example, from an NLOS to an LOS situation, or from an open place in a city

into a narrow street. Consequently, new transceiver concepts should always also be verified by using channel measurements in the appropriate system deployment scenarios such as high-speed public access scenarios (e.g., access point to car), public open indoor areas (e.g., airport), or factory halls. The acquired data can afterwards be used in offline simulations for comparing even completely different transceiver architectures with exact reproducibility.

Developing the new wireless networks beyond 3G may require the consideration of completely new transceiver constellations, for example, multihop systems, distributed multi-antenna systems, and tandem air interfaces. The presented performance evaluation methodology can be extended to enable reliable propagation modeling also for such configurations. Furthermore, the consideration of network aspects by measurement-based system-level simulations is possible if simultaneous measurements from multiple sites in a certain radio environment are carried out.

Two different methods for measurement-based MIMO channel modeling have been presented and compared. Their application to the performance evaluation of the turbo-MIMO equalizer concept revealed a reasonable performance in many real field scenarios, but also a sensitivity to the propagation conditions. The observed results suggest that advanced link adaptation algorithms are required to prevent excessive BERs. The causality of certain performance effects can be traced back to the instantaneous channel conditions by referring to the results of a propagation analysis, either by high-resolution estimation of multipath parameters or by nonparametric statistical investigations. This provides significant insights both for the verification and enhancement of channel models and for the optimization of particular Tx and Rx signal processing schemes. Moreover, the described methods provide exceptional opportunities for investigating adequate link adaptation criteria and strategies.

According to the opinion of the authors, realistic channel modeling in MIMO systems is presently only possible with a balanced mix of a deterministic modeling approach for representative scenarios and the frequently favored stochastic modeling approaches. Only this allows to identify the relevant factors influencing the transceiver performance. In this context, a real-time MIMO channel sounder is a valuable component of a rapid prototyping system when developing new physical layer principles. A complete framework for measurement-based simulations comprises besides the measurement equipment a tool chain for measurement data archiving, data handling, and propagation analysis. The huge potential of measurement-based methods for fast and reliable performance evaluation has not yet been fully recognized in industry but the acceptance is growing.

ACKNOWLEDGMENTS

REFERENCES

[1] G. J. Foschini and M. J. Gans, "On limits of wireless personal communications in a fading environment when using multiple antennas," *Wireless Personal Communications*, vol. 6, no. 3, pp. 311–335, 1998.

[2] R. S. Thomä, D. Hampicke, A. Richter, G. Sommerkorn, and U. Trautwein, "MIMO vector channel sounder measurement for smart antenna system evaluation," *European Transactions on Telecommunications*, vol. 12, no. 5, pp. 427–438, 2001.

[3] D. Gesbert, M. Shafi, D. Shiu, P. J. Smith, and A. Naguib, "From theory to practice: an overview of MIMO space-time coded wireless systems," *IEEE J. Select. Areas Commun.*, vol. 21, no. 3, pp. 281–302, 2003.

[4] B. M. Hochwald and S. ten Brink, "Achieving near-capacity on a multiple-antenna channel," *IEEE Trans. Commun.*, vol. 51, no. 3, pp. 389–399, 2003.

[5] G. Raleigh and J. M. Cioffi, "Spatio-temporal coding for wireless communication," *IEEE Trans. Commun.*, vol. 46, no. 3, pp. 357–366, 1998.

[6] A. J. Paulraj and C. B. Papadias, "Space-time processing for wireless communications," *IEEE Signal Processing Mag.*, vol. 14, no. 6, pp. 49–83, 1997.

[7] S. Lek, "Turbo space-time processing to improve wireless channel capacity," *IEEE Trans. Commun.*, vol. 48, no. 8, pp. 1347–1359, 2000.

[8] M. Moher, "An iterative multiuser decoder for near-capacity communications," *IEEE Trans. Commun.*, vol. 46, no. 7, pp. 870–880, 1998.

[9] X. Wang and H. V. Poor, "Iterative (turbo) soft interference cancellation and decoding for coded CDMA," *IEEE Trans. Commun.*, vol. 47, no. 7, pp. 1046–1061, 1999.

[10] M. C. Reed, C. B. Schlegel, P. D. Alexander, and J. A. Asenstorfer, "Iterative multiuser detection for CDMA with FEC: near-single-user performance," *IEEE Trans. Commun.*, vol. 46, no. 12, pp. 1693–1699, 1998.

[11] T. Abe and T. Matsumoto, "Space-time turbo equalization in frequency-selective MIMO channels," *IEEE Trans. Veh. Technol.*, vol. 52, no. 3, pp. 469–475, 2003.

[12] D. Gesbert, H. Bölcskei, D. A. Gore, and A. J. Paulraj, "Outdoor MIMO wireless channels: models and performance prediction," *IEEE Trans. Commun.*, vol. 50, no. 12, pp. 1926–1934, 2002.

[13] H. Özcelik, M. Herdin, W. Weichselberger, J. Wallace, and E. Bonek, "Deficiencies of 'Kronecker' MIMO radio channel model," *Electronics Letters*, vol. 39, no. 16, pp. 1209–1210, 2003.

[14] U. Trautwein, T. Matsumoto, C. Schneider, and R. S. Thomä, "Exploring the performance of turbo MIMO equalization in real field scenarios," in *Proc. 5th International Symposium on Wireless Personal Multimedia Communications (WPMC '02)*, vol. 2, pp. 422–426, Honolulu, Hawaii, USA, October 2002.

[15] D. Reynolds and X. Wang, "Low complexity turbo-equalization for diversity channels," *Signal Processing*, vol. 81, no. 5, pp. 989–995, 2001.

[16] A. Dejonghe and L. Vandendorpe, "Turbo equalization for multilevel modulation: a low complexity approach," in *Proc. IEEE International Conference on Communications (ICC '02)*, vol. 3, pp. 1863–1867, New York, NY, USA, April–May 2002.

[17] S. ten Brink, J. Speidel, and R.-H. Yan, "Iterative demapping and decoding for multilevel modulation," in *Proc. IEEE Global Telecommunications Conference (GLOBECOM '98)*, vol. 1, pp. 579–584, Sydney, NSW, Australia, November 1998.

[18] M. Steinbauer, A. F. Molisch, and E. Bonek, "The double-directional radio channel," *IEEE Antennas Propagat. Mag.*, vol. 43, no. 4, pp. 51–63, 2001.

[19] R. S. Thomä, D. Hampicke, M. Landmann, A. Richter, and S. Sommerkorn, "Measurement-based parametric channel modelling (MBPCM)," in *Proc. International Conference on Electromagnetics in Advanced Applications (ICEAA '03)*, Torino, Italy, September 2003.

[20] H. Xu, D. Chizhik, H. Huang, and R. Valenzuela, "A wave-based wideband MIMO channel modeling technique," in *Proc. 13th IEEE International Symposium on Personal, Indoor, and Mobile Radio Communications (PIMRC '02)*, vol. 4, pp. 1626–1630, Lisbon, Portugal, September 2002.

[21] K. Yu and B. Ottersten, "Models for MIMO propagation channels: a review," *Wireless Communications and Mobile Computing*, vol. 2, no. 7, pp. 653–666, 2002, Special Issue on "Adaptive Antennas and MIMO Systems".

[22] A. F. Molisch, "A generic model for MIMO wireless propagation channels in macro- and microcells," *IEEE Trans. Signal Processing*, vol. 52, no. 1, pp. 61–71, 2004.

[23] http://www.channelsounder.de.

[24] R. S. Thomä, M. Landmann, and A. Richter, "RIMAX—A maximum likelihood framework for parameter estimation in multidimensional channel sounding," in *Proc. International Symposium on Antennas and Propagation (ISAP '04)*, pp. 53–56, Sendai, Japan, August 2004.

[25] A. Richter and R. S. Thomä, "Parametric modelling and estimation of distributed diffuse scattering components of radio channels," COST 273 TD(03)198, Prague, Czech Republic, Septemper 2003, http://www.lx.it.pt/cost273/.

[26] P. Robertson, E. Villebrun, and P. Hoeher, "A comparison of optimal and sub-optimal MAP decoding algorithms operating in the log-domain," in *Proc. IEEE International Conference on Communications (ICC '95)*, vol. 2, pp. 1009–1013, Seattle, Wash, USA, June 1995.

[27] C. Schneider, R. S. Thomä, U. Trautwein, and T. Matsumoto, "The dependency of turbo MIMO equalizer performance on the spatial and temporal multipath channel structure—a measurement based evaluation," in *Proc. IEEE 57th Semiannual Vehicular Technology Conference (VTC '03)*, vol. 2, pp. 808–812, Jeju, South Korea, April 2003.

Uwe Trautwein received the Dipl.-Ing. degree in electrical engineering from Ilmenau University of Technology, Germany, in 1993. From 1994 to 1999, he was a Research Assistant at the Institute of Communications and Measurement Engineering, Ilmenau University of Technology. From 1999 to 2001 he worked as a Scientific Associate at the Institute for Microelectronics and Mechatronics Systems (IMMS), Ilmenau. Since 2001, he has been with ME-DAV/TeWiSoft in Ilmenau. In 1994 and 1999, respectively, he was a Visiting Researcher for several months at the Institute of Communications and Radio Frequency Engineering, Vienna University of Technology, Austria, and at the NTT DoCoMo Wireless Laboratory at YRP, Yokosuka, Japan. His research interests are in the areas of signal processing for wireless communications, statistical signal analysis, space-time methods, radio channel measurement and modeling, and simulation methodology.

Christian Schneider received his Diploma degree in electrical engineering from the Technische Universität Ilmenau, Ilmenau, Germany, in 2001. He is currently pursuing the Dr.-Ing. degree at the Electronic Measurement Research Lab, the Institute of Communications and Measurement Engineering, the Ilmenau University of Technology. His research interests include space-time signal processing, turbo techniques, multidimensional channel sounding, channel characterization, and channel modeling.

Reiner Thomä received the Dipl.-Ing. (M.S.E.E.), Dr.-Ing. (Ph.D.E.E.), and the Dr.-Ing. habil. degrees in electrical engineering (information technology) from Technische Hochschule Ilmenau, Germany, in 1975, 1983, and 1989, respectively. From 1975 to 1988, he was a Research Associate in the fields of electronic circuits, measurement engineering, and digital signal processing at the same university. From 1988 to 1990, he was a Research Engineer at the Akademie der Wissenschaften der DDR (Zentrum für Wissenschaftlichen Gerätebau). During this period, he was working in the field of radio surveillance. In 1991, he spent a three-month sabbatical leave at the University of Erlangen-Nürnberg (Lehrstuhl für Nachrichtentechnik). Since 1992, he has been a Professor of electrical engineering (electronic measurement) at TU Ilmenau where he has been the Director of the Institute of Communications and Measurement Engineering since 1999. His research interests include measurement and digital signal processing methods (correlation and spectral analysis, system identification, array methods, time-frequency and cyclostationary signal analysis), their application in mobile radio and radar systems (multidimensional channel sounding, propagation measurement and parameter estimation, ultra-wideband radar), and measurement-based performance evaluation of MIMO transmission systems.